Irreversible Reactions and Diffusive Escape: Stationary Properties

P. L. Krapivsky[1] and E. Ben-Naim[2]

[1]*Department of Physics, Boston University, Boston, Massachusetts 02215*
[2]*Theoretical Division and Center for Nonlinear Studies,*
Los Alamos National Laboratory, Los Alamos, New Mexico 87545

We study three basic diffusion-controlled reaction processes—annihilation, coalescence, and aggregation. We examine the evolution starting with the most natural inhomogeneous initial configuration where a half-line is uniformly filled by particles, while the complementary half-line is empty. We show that the total number of particles that infiltrate the initially empty half-line is finite and has a stationary distribution. We determine the evolution of the average density from which we derive the average total number N of particles in the initially empty half-line; e.g., for annihilation $\langle N \rangle = \frac{3}{16} + \frac{1}{4\pi}$. For the coalescence process, we devise a procedure that in principle allows one to compute $P(N)$, the probability to find exactly N particles in the initially empty half-line; we complete the calculations in the first non-trivial case ($N = 1$). As a by-product we derive a distance distribution between the two leading particles.

I. INTRODUCTION

Reaction-diffusion systems are ubiquitous in biology, chemistry and physics. An important class of such systems, diffusion-controlled processes in which a reaction happens whenever two reactants "meet", has been studied for almost a century (see e.g. [1–13]). Mathematically, these processes are strongly interacting infinite particle systems, so it is not surprising that many basic questions remain unanswered. Here we analyze a few basic diffusion-controlled processes focusing on the interplay between reaction and spatial inhomogeneity of the initial setting. We will see that for an extreme inhomogeneous initial configuration with an empty half-line (1), the statistics of the occupation number of this half-line is asymptotically stationary and highly non-trivial.

We study three diffusion-controlled reaction systems. One is a single-species annihilation which is represented by the reaction scheme

$$A + A \to \emptyset \tag{1}$$

Identical particles (denoted by A) undergo diffusion and whenever two particles touch each other, they disappear. Strict annihilation is rare. One example is the annihilation of domain walls in an Ising spin chain subjected to a zero-temperature spin-flip dynamics [13]. In most situations, however, annihilation merely implies that the reaction product does not further affect the reaction process. For instance, a collision between two atoms may lead to the formation of a diatomic molecule; if such molecules are stable (that is, they do not break back to atoms) and if they do not influence diffusing atoms, we can effectively ignore the molecules and use the reaction scheme (1).

Another simple diffusion-controlled process, coalescence, can be represented by the reaction scheme

$$A + A \to A \tag{2}$$

Strict coalescence is also rare. It occurs for example in a Potts chain with infinitely many states evolving ac-
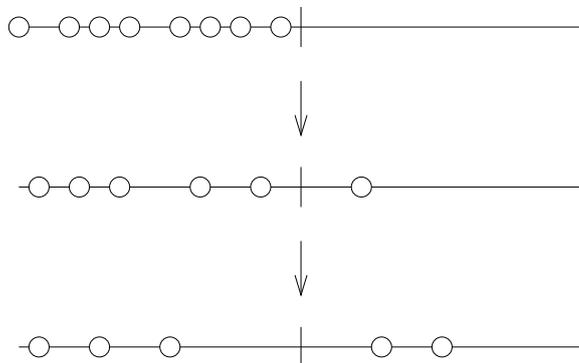

FIG. 1: Illustration of the irreversible reaction process. The initial condition with fixed concentration of particles left of the origin and no particles to the right of the origin is shown on the top. The next two layers illustrate the state of the system at later times (the latest time at the bottom) with a dwindling concentration of particles left of the origin and a fluctuating *finite* total number of particles to the right of the origin.

cording to the non-conserved zero-temperature dynamics [13]. In most situations, the coalescence process is a coarse-grained description of the aggregation process

$$A_i + A_j \to A_{i+j} \tag{3}$$

where A_m represents clusters of mass m, i.e., clusters composed of m monomers. The symbolic representation (2) indicates that we disregard the mass of aggregates and hence it faithfully describes the gross features of the aggregation process when the diffusion constant is mass-independent and when the size is also mass-independent (or the size is irrelevant as in one dimension).

Little is known about evolution of irreversible reactions starting from spatially inhomogeneous configurations. Here we consider the simplest situation when at time $t = 0$ the half space $x < 0$ is uniformly filled by

particles, while the half space $x > 0$ is empty (see Fig. 1)

$$c(x, t = 0) = \begin{cases} \rho & x < 0 \\ 0 & x > 0 \end{cases} \qquad (4)$$

This step-function initial condition has been used e.g. to study front propagation in reaction-diffusion processes [14, 15] and shock waves in driven exclusion processes [16], it is also popular in experimental [17, 18] and theoretical (see e.g. [19–22]) studies of cold quantum gases, and in analyses of quantum spin chains ([23–26] and references therein).

In three dimensions, one can use the rate equation approach to analyze the evolution. For annihilation and coalescence processes, the density $c(x, t)$ satisfies the reaction-diffusion equation, $\partial_t c = D \partial_{xx} c - K c^2$, where D is the diffusion coefficient and K the reaction rate. The long time behavior is simple, viz. in the scaling limit

$$|x| \to \infty, \quad t \to \infty, \quad X = \frac{x}{\sqrt{2Dt}} = \text{finite}, \qquad (5)$$

the density becomes $c(x, t) = (Kt)^{-1} C(X)$. The scaled density $C(X)$ satisfies an ordinary differential equation which can be solved numerically.

In this paper we focus on the one-dimensional case. This is the most challenging setting and the emergent results are richer than in higher dimensions. The challenge stems from the fact that in one dimension one cannot employ the rate equation approach, i.e., one cannot rely on reaction-diffusion equations. The behaviors are still well understood when the initial conditions are homogeneous, e.g., $c \sim (Dt)^{-1/2}$, see e.g. [6, 7, 12, 13]. For the inhomogeneous initial condition (Fig. 1) the density eventually decays in the same manner everywhere. However, particles infiltrate only up to distance $\sim \sqrt{Dt}$ into the vacant half-line, so the total *number* of particles in the initially vacant half-line is expected to be finite and governed by a stationary distribution. In this paper, we establish this behavior analytically.

For the inhomogeneous setting (4), the scaling form

$$c(x, t) = \frac{1}{\sqrt{2\pi Dt}} C(X) \qquad (6)$$

is anticipated. We shall obtain the scaled density profile $C(X)$ analytically. An immediate consequence of (6) is that the average total number of particles $\langle N \rangle$ in the initially empty half-line is *finite*. More precisely, for the coalescence process

$$\langle N \rangle_c = \frac{3}{8} + \frac{1}{2\pi} = 0.534154943 \ldots \qquad (7)$$

For the annihilation process, the value is twice smaller. Thus the total number of particles N in the initially empty half-line is a fluctuating quantity with a finite average. (The total number of particles in the initially filled half-line is of course infinite, although the density vanishes algebraically with time $\sim (Dt)^{-1/2}$.) Furthermore,

we also find that the total number of particles N is governed by a stationary probability distribution $P(N)$.

The determination $P_c(N)$ for the coalescence process is technically challenging. In addition to $P_c(0) = \frac{1}{2}$ which can be established on the basis of symmetry alone, we are able to compute the probability

$$\begin{aligned} P_c(1) &= \frac{11\pi - 4}{16\pi} + \frac{1}{2\pi}\left[\arctan\left(\frac{1}{\sqrt{8}}\right) - 2\arctan\left(\frac{1}{\sqrt{2}}\right)\right] \\ &= 0.466095976 \ldots \end{aligned} \qquad (8)$$

to have exactly one particle in the initially empty half-line. With much more effort it could be possible to determine $P_c(2)$, but to find the entire distribution $P_c(N)$ requires more advanced methods.

For the annihilation process we haven't been able even to determine $P_a(0)$. Indeed, the coalescence process is more tractable than the annihilation process. This subtle difference between these two very similar diffusion-controlled reaction processes was already encountered in the homogeneous setting. For instance, for the coalescence process the distance distribution between adjacent particles is well-known (see [12, 13]), while for the annihilation process the distance distribution has not been determined analytically [27–29]. Another long-standing unresolved problem is to determine the long-time behavior of an impurity (a particle with diffusion coefficient generally different from the diffusion coefficient of the host particles) in the annihilation process [30, 31].

The annihilation process in the half-filled setting (4) was introduced in [32]. That study focused on the survival probabilities $S_n(t)$, where $n = 1, 2, \ldots$ labels particles according to their initial locations: $x_1(0) > x_2(0) > x_3(0)$ etc. These survival probabilities exhibit an intriguing temporal behavior, the decay laws depend only on the parity of the original label: $S_n \sim t^{-\alpha}$ for even n and as $S_n \sim t^{-\beta}$ for odd n; the decay exponents α and β are still unknown [32].

The rest of this article is organized as follows. In Sec. II we consider diffusion-controlled annihilation, coalescence, and aggregation processes in one dimension and compute the average densities everywhere. Statistics of the total number of particles in the initially empty half-line is studied in Sec. III. In Sec. IV we summarize our results and discuss several open problems.

II. DENSITY PROFILE

In one dimension, we compute the density profile using the empty interval method which allows an efficient analytical treatment of the one-dimensional diffusion-controlled coalescence process (Sec. II A). Modifications of the empty interval method which are suitable for annihilation and aggregation are presented in Sec. II B and Sec. II C.

We consider continuous versions of the aggregation, annihilation and coalescence processes in which size-less particles undergo Brownian motions on a line. Lattice

versions in which each particle occupies a site on the one-dimensional lattice and hops to nearest-neighboring sites are also tractable. The basic asymptotic behaviors are identical in both versions.

A. Coalescence Process

In the one-dimensional diffusion-controlled coalescence process, point particles undergo identical independent Brownian motions and merge instantaneously whenever they meet. An elegant exact treatment of this strongly interacting infinite particle system is possible through the empty interval technique [10, 12, 13, 27, 33–35].

To explain the empty interval technique, we begin with spatially-homogeneous coalescence process. Let $E(x, y; t)$ be the probability that the interval $[x, y]$ is empty at time t. In the homogeneous case these probabilities depend only on the length of the interval: $E(x, y; t) = E(\ell, t)$ where $\ell = y - x$. The probabilities $E(\ell, t)$ satisfy the diffusion equation

$$\frac{\partial E(\ell, t)}{\partial t} = 2D \frac{\partial^2 E(\ell, t)}{\partial \ell^2} \qquad (9)$$

and the boundary condition

$$E(\ell = 0, t) = 1 \qquad (10)$$

The initial condition is $E(\ell, t = 0) = e^{-\rho \ell}$ if the initial distribution of particles is random and the initial density is ρ. Note also the general formula for the concentration

$$c(t) = -\frac{\partial E(\ell, t)}{\partial \ell}\bigg|_{\ell=0} \qquad (11)$$

The physically relevant region is $\ell \geq 0$, but we can extend (9) to $\ell < 0$. It proves convenient to make a shift, $F(\ell, t) = E(\ell, t) - 1$, so that the boundary condition (10) becomes $F(\ell = 0, t) = 0$. The governing equation for $F(\ell, t)$ remains the diffusion equation

$$\frac{\partial F}{\partial t} = 2D \frac{\partial^2 F}{\partial \ell^2} \qquad (12)$$

We have $F(\ell, t = 0) = e^{-\rho \ell} - 1$ when $\ell > 0$ and we seek the initial condition for $\ell < 0$ in such a way that the boundary condition $F(\ell = 0, t) = 0$ is manifestly obeyed. The proper choice is

$$F(\ell, t = 0) = \begin{cases} \exp[-\rho \ell] - 1 & \ell > 0 \\ 1 - \exp[\rho \ell] & \ell < 0 \end{cases} \qquad (13)$$

One can write an exact solution of the diffusion equation (12) subject to the initial condition (13). We do not display this solution since our main goal is to establish the long-time behavior, and for that purpose, we can replace (13) by the simplified initial condition

$$F(\ell, t = 0) = \begin{cases} -1 & \ell > 0 \\ 1 & \ell < 0 \end{cases} \qquad (14)$$

The solution to (12) and (14) is $F = -\text{Erf}(\ell/\sqrt{8Dt})$, and therefore

$$E(\ell, t) = \text{Erfc}\left(\frac{\ell}{\sqrt{8Dt}}\right) \qquad (15)$$

By combining (11) and (15) we recover the long-time asymptotic behavior of the density

$$c(t) = \frac{1}{\sqrt{2\pi Dt}} \qquad (16)$$

We now turn to the spatially-inhomogeneous initial condition (4). The mathematical formulation is a natural generalization of Eqs. (9)–(11). The governing equations are

$$\frac{\partial}{\partial t} E(x, y; t) = D \left(\frac{\partial^2}{\partial x^2} + \frac{\partial^2}{\partial y^2}\right) E(x, y; t) \qquad (17)$$

The boundary condition becomes

$$E(x, x; t) = 1 \qquad (18)$$

The density is found from

$$c(x, t) = -\frac{\partial E(x, y; t)}{\partial y}\bigg|_{y=x} \qquad (19)$$

We have to solve (17) subject to the initial condition

$$E_0(x, y) = \begin{cases} 1 & 0 < x < y \\ \exp[\rho x] & x < 0 < y \\ \exp[\rho(x - y)] & x < y < 0 \end{cases} \qquad (20)$$

Writing $E(x, y; t) = 1 + F(x, y; t)$ and focusing on the long-time limit we can again use a simplified initial condition:

$$F_0(x, y) = \begin{cases} 0 & 0 < \min(x, y) \\ -1 & x < 0, \ x < y \\ 1 & y < 0, \ y < x \end{cases} \qquad (21)$$

Changing variables

$$\xi = y + x, \quad \eta = y - x \qquad (22)$$

we end up with the two-dimensional diffusion equation

$$\frac{\partial}{\partial t} F(\xi, \eta; t) = 2D \left(\frac{\partial^2}{\partial \xi^2} + \frac{\partial^2}{\partial \eta^2}\right) F(\xi, \eta; t) \qquad (23)$$

subject to the initial condition [Fig. 2]

$$F_0(\xi, \eta) = \begin{cases} 0 & 0 < \xi, \ -\xi < \eta < \xi \\ -1 & 0 < \eta, \ \xi < \eta \\ 1 & \eta < 0, \ \xi < -\eta \end{cases} \qquad (24)$$

Expressing the boundary condition (18) in terms of the auxiliary function $F(\xi, \eta; t)$ gives $F(\xi, \eta = 0; t) = 0$. This
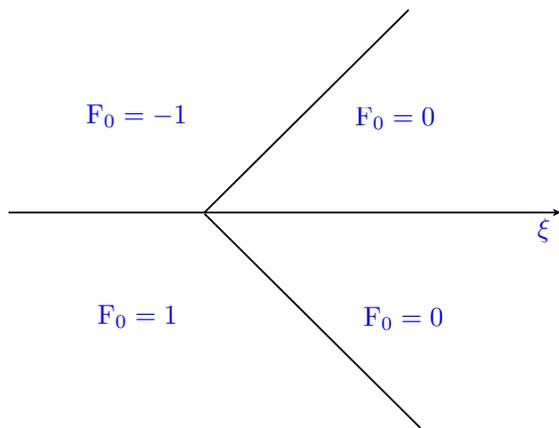
FIG. 2: The initial condition $F_0(\xi, \eta) = F(\xi, \eta; t = 0)$ in the (ξ, η) plane. The vanishing of $F(\xi, \eta; t)$ on the ξ axis, $F|_{\eta=0} = 0$, is manifest.

boundary condition is indeed manifestly obeyed with the choice of initial condition (24), see Fig. 2.

The solution to equation (23)–(24) is straightforward. One gets

$$
\begin{aligned}
E(x, y; t) &= 1 - \tfrac{1}{2}\mathrm{Erfc}\left(\tfrac{X+Y}{2}\right)\mathrm{Erf}\left(\tfrac{Y-X}{2}\right) \\
&- \frac{1}{\pi}\int_{-\frac{X+Y}{2}}^{\infty} du\, e^{-u^2}\int_{u+X}^{u+Y} dv\, e^{-v^2} \quad (25)
\end{aligned}
$$

where $X = x/\sqrt{2Dt}$ and $Y = y/\sqrt{2Dt}$. By substituting (25) into (19) we confirm the scaling form (6) and obtain the density profile

$$
C(X) = \frac{1}{2}\mathrm{Erfc}(X) + \frac{1}{\sqrt{8}}\,e^{-X^2/2}\,\mathrm{Erfc}\left(-\frac{X}{\sqrt{2}}\right) \quad (26)
$$

The density profile (26) holds everywhere and it does *not* depend on the initial density ρ. The latter property is known in the homogeneous case, so it must hold when $X \to -\infty$; remarkably, it remains true even for the initially empty half-line. The dependence on the initial density can be observed e.g. for $x \sim t$, but for any fixed X this dependence disappears in the long time limit.

On the interface separating the two half-lines, we have $C(X = 0) = \frac{1}{2} + \frac{1}{\sqrt{8}} = 0.853553\ldots$ (see Fig. 3). If there were no reactions, only diffusion, $c(x, t) = \frac{1}{2}\mathrm{Erfc}\left(\frac{X}{\sqrt{2}}\right)$, so on the interface separating the two half spaces the density is exactly a half that of the bulk.

The exact solution (25) contains information beyond the density. For instance, specializing (25) to $Y = \infty$ gives the probability $\mathcal{E}(x; t) \equiv E(x, y = \infty; t)$ that the half-line (x, ∞) is empty. This probability is the function of a single scaled variable:

$$
\mathcal{E}(x; t) = \mathcal{E}(X) = 1 - \frac{1}{2\sqrt{\pi}}\int_{-\infty}^{\infty} du\, e^{-u^2}\,\mathrm{Erfc}(u + X)
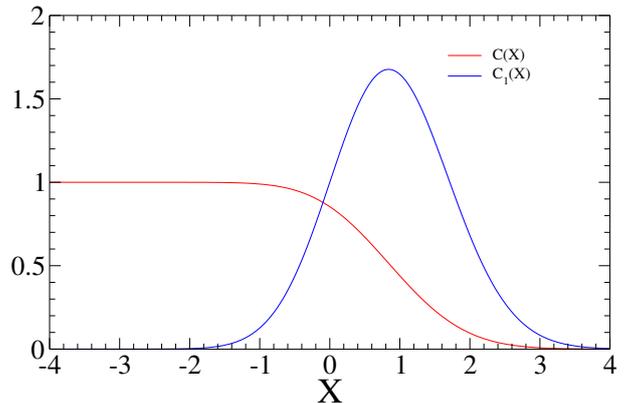$$

FIG. 3: The scaled density $C(X)$ in all three processes and the scaled density of monomers $C_1(X)$ for the aggregation process. The density $C(X)$ is the same, Eq. (26), both for the coalescence and annihilation processes if the scaling forms are chosen according to (6) for the coalescence process and (31) for the annihilation process. In the aggregation process, the scaled densities of clusters of small mass are given by the same Eq. (40) as the density of monomers.

The integral can be expressed through the error function:

$$
\mathcal{E}(X) = 1 - \frac{1}{2}\mathrm{Erfc}\left(\frac{X}{\sqrt{2}}\right) \quad (27)
$$

The behavior $\mathcal{E}(0) = \frac{1}{2}$ simply reflects that the right-most particle in the coalescence process is equally likely to be to the left and to the right of the origin [see also (46)].

B. Irreversible Annihilation Process

For the irreversible annihilation process (1), instead of empty interval probabilities one considers $G(x, y; t)$, the probability that there is an even number of particles in the interval $[x, y]$. The probabilities $G(x, y; t)$ satisfy the same equations (17)–(19) as the empty interval probabilities (see [27, 35]), the only difference is the initial condition, viz. instead of (20) one gets

$$
G_0(x, y) = \frac{1}{2} + \frac{1}{2}\times
\begin{cases}
1 & 0 < x < y \\
\exp[2\rho x] & x < 0 < y \\
\exp[2\rho(x - y)] & x < y < 0
\end{cases}
$$

There is therefore a duality between annihilation and coalescence, namely

$$
G(x, y; t) = \tfrac{1}{2} + \tfrac{1}{2}E(x, y; t) \quad (28)
$$

This duality holds if the initial densities differ by factor 2 exactly:

$$
\rho^{\mathrm{annihilation}} = \tfrac{1}{2}\rho^{\mathrm{coalescence}} \quad (29)
$$

This remarkable duality between annihilation and coalescence extends to more complicated correlation functions. It was found [35–39] in the context of homogeneous setting, and it also holds also for our spatially-inhomogeneous setting.

In the long-time limit, the initial densities are irrelevant, to leading order, and therefore, we have

$$G(x,y;t) = 1 - \tfrac{1}{4}\text{Erfc}\left(\tfrac{X+Y}{2}\right)\text{Erf}\left(\tfrac{Y-X}{2}\right)$$
$$- \frac{1}{2\pi}\int_{-\frac{X+Y}{2}}^{\infty} du\, e^{-u^2}\int_{u+X}^{u+Y} dv\, e^{-v^2} \quad (30)$$

The density has the scaling form

$$c_a(x,t) = \frac{1}{\sqrt{8\pi Dt}}\, C(X) \quad (31)$$

with the same scaled density $C(X)$ as before, Eq. (26).

Specializing (30) to $Y = \infty$ gives the probability $\mathcal{E}_a(x;t) \equiv G(x,y=\infty;t)$ that the half-line (x,∞) contains an even number of particles:

$$\mathcal{E}_a(X) = 1 - \frac{1}{4\sqrt{\pi}}\int_{-\infty}^{\infty} du\, e^{-u^2}\text{Erfc}(u+X) \quad (32)$$

In particular, the initially-empty half line contains an even number of particles with probability

$$\mathcal{E}_a(0) = \sum_{N\geq 0} P_a(2N) = \frac{3}{4} \quad (33)$$

C. Irreversible Aggregation Process

The average mass density $\mu(x,t) = \sum_{m\geq 1} m c_m(x,t)$ is not affected by the aggregation process and hence it satisfies the diffusion equation $\partial_t \mu = D\partial_{xx}\mu$. Therefore

$$\mu(x,t) = \frac{\rho}{2}\text{Erfc}\left(\frac{x}{\sqrt{4Dt}}\right) = \frac{\rho}{2}\text{Erfc}\left(\frac{X}{\sqrt{2}}\right) \quad (34)$$

To probe other average characteristics, we need more advanced methods. It turns out [33, 34] that instead of empty interval probabilities it suffices to use $P_m(x,y;t)$, the probability that the total mass inside the interval $[x,y]$ equals m. Assuming that all clusters are point particles that diffuse with the same diffusion constant D, one finds that the probabilities $P_m(x,y;t)$ satisfy

$$\frac{\partial}{\partial t}P_m(x,y;t) = D\left(\frac{\partial^2}{\partial x^2} + \frac{\partial^2}{\partial y^2}\right)P_m(x,y;t) \quad (35)$$

The boundary condition (18) generalizes to

$$P_m(x,x;t) = \delta_{m,0} \quad (36)$$

The mass distribution is found from

$$c_m(x,t) = \frac{\partial P_m(x,y;t)}{\partial y}\bigg|_{y=x} \quad (37)$$

The initial condition reads

$$P_m(t=0) = \begin{cases} \delta_{m,0} & 0 < x < y \\ \frac{(\rho|x|)^m}{m!}e^{\rho x} & x < 0 < y \\ \frac{[\rho(y-x)]^m}{m!}e^{\rho(x-y)} & x < y < 0 \end{cases} \quad (38)$$

The governing equations (35) are linear, yet their analysis is rather cumbersome, see Appendix A. Here we just present the major findings. In the scaling limit (5), the mass distribution acquires the scaling form

$$c_m(X,t) = \frac{1}{4\pi\rho Dt}\, C_m(X) \quad (39)$$

For $m = O(1)$, the scaled densities become mass independent, i.e., the same as the monomer density

$$C_m(X) = \sqrt{\frac{\pi}{2}}\, X e^{-X^2/2}\text{Erfc}\left(-\frac{X}{\sqrt{2}}\right) + e^{-X^2} \quad (40)$$

As a function of the scaled distance, the monomer density has a single peak (Fig. 3) and it is maximal at $X \approx 0.84$.

One anticipates that the mass density $C_m(X)$ depends on the scaled mass:

$$C_m(X) = \Phi(M,X), \qquad M = \frac{m}{\rho\sqrt{2\pi Dt}} \quad (41)$$

We now use the sum rule $\sum_{m\geq 1} c_m(X,t) = c(X,t)$, the scaled mass distribution (39), (41) together with the cluster density (6) to obtain an integral relation for the scaled mass density

$$\int_0^{\infty} dM\, \Phi(M,X) = \text{Erfc}(X) + \frac{e^{-X^2/2}}{\sqrt{2}}\text{Erfc}\left(-\frac{X}{\sqrt{2}}\right) \quad (42)$$

Similarly the sum rule $\sum_{m\geq 1} m c_m(X,t) = \mu(X,t)$ together with the exact result (34) for the mass density lead to another integral relation

$$\int_0^{\infty} dM\, M\Phi(M,X) = \text{Erfc}\left(\frac{X}{\sqrt{2}}\right) \quad (43)$$

The small mass tail of $\Phi(M,X)$ is given by (40); it would be interesting to derive the large mass tail.

III. PARTICLE NUMBER

Here we study the total number of particles $N(t)$ that infiltrate the initially empty half-line. This natural quantity is *finite*, and it fluctuates throughout the evolution. Hence, the average does not fully characterize its probability distribution function. The finiteness of $N(t)$ follows from the following heuristic argument. The decay law $c \sim (Dt)^{-1/2}$ in the homogeneous case and the fact that particles spread at most by distance $\sqrt{Dt}$ into initially empty half-line suggest that N is indeed of the order of one. We can actually compute the average total number

of particles $\langle N \rangle$ in the initially empty half-line. For the coalescence process, we use (6) to obtain

$$\langle N \rangle_{\rm c} = \int_0^\infty dx\, c(x,t) = \frac{1}{\sqrt{\pi}} \int_0^\infty dX\, C(X) \qquad (44)$$

which in conjunction with the density profile (26) leads to the announced result (7). For the annihilation process, the density is exactly two times smaller; accordingly, the average total number of particles is

$$\langle N \rangle_{\rm a} = \frac{3}{16} + \frac{1}{4\pi} = 0.267077471\ldots \qquad (45)$$

To learn more about the random quantity N, one needs to compute its probability distribution $P(N)$. The distribution functions for the reaction processes (1) and (2) are actually different. We are interested in both $P_{\rm c}(N)$ and $P_{\rm a}(N)$. (We distinguish the two cases with subscripts.) The coalescence process is simpler, and a few exact results are possible.

The simplest exact result is the probability of finding no particles in the initially empty half-line:

$$P_{\rm c}(0) = \frac{1}{2} \qquad (46)$$

The probability to find exactly one particle in the initially empty half-line is given by (8) as we show below. The derivation of this result (Sec. III A) is quite involved. In contrast, Eq. (46) is easy to establish. Consider the right-most particle R and notice that from its 'view-point' the coalescence process (2) reduces to $A + R \to R$, that is, the right-most particle is not affected at all, so it undergoes one-dimensional Brownian motion. In the long-time limit, the diffusing particle will be in the left-half space with the same probability $\frac{1}{2}$ as in the right-half space. The right-most particle is in the left-half space, $x < 0$, is equivalent to saying that $N = 0$. This establishes (46).

The normalization requirement, $\sum_{N \geq 0} P_{\rm c}(N) = 1$, together with (46) indicates that $\sum_{N \geq 1} P_{\rm c}(N) = \frac{1}{2}$. Combining this result with $\langle N \rangle_{\rm c} = \sum_{N \geq 1} N P_{\rm c}(N)$ and Eq. (7) we obtain the sum rule

$$\sum_{N \geq 2} (N-1) P_{\rm c}(N) = \frac{1}{2\pi} - \frac{1}{8} = 0.0341549431\ldots \qquad (47)$$

This sum rule leads to the upper bound for the probability to find two particles:

$$P_{\rm c}(2) < 0.0341549431\ldots \qquad (48)$$

Combining the normalization requirement with (46) and (8) we similarly derive the sum rule

$$\begin{aligned}\sum_{N \geq 3} (N-2) P_{\rm c}(N) &= \frac{1}{16} + \frac{1}{4\pi} \\ &\quad + \frac{1}{2\pi}\left[\arctan\left(\frac{1}{\sqrt{8}}\right) - 2\arctan\left(\frac{1}{\sqrt{2}}\right)\right] \\ &= 0.00025091951\ldots\end{aligned}$$

which yields the upper bound for the probability to find three particles in the initially empty half-line:

$$P_{\rm c}(3) < 0.00025091951\ldots \qquad (49)$$

A. Computation of $P_{\rm c}(1)$

We now consider the coalescence process and show that the probability $P_{\rm c}(1)$ to have exactly one particle in the initially empty half-line is given by (8). In principle, our procedure can be extended to $P_{\rm c}(N)$ with arbitrary N; yet the computation quickly becomes prohibitive.

To determine $P_{\rm c}(1)$ we use probabilities for two intervals to be empty. In Sec. II A we computed the probability $E(x,y)$ that the interval (x,y) is empty at time t. (In the following we do not display the time variable, so $E(x,y)$ denotes $E(x,y|t)$, etc.) Let $E(x_1,y_1;x_2,y_2)$ be the probability that the intervals (x_1,y_1) and (x_2,y_2) are empty. We shall assume that $x_1 < y_1 < x_2 < y_2$, so the intervals are non-overlapping. The probability $E(1;2) \equiv E(x_1,y_1;x_2,y_2)$ satisfies

$$\frac{\partial}{\partial t} E(1;2) = D\left(\frac{\partial^2}{\partial x_1^2} + \frac{\partial^2}{\partial y_1^2} + \frac{\partial^2}{\partial x_2^2} + \frac{\partial^2}{\partial y_2^2} \right) E(1;2)$$

The solution of this equation, with obvious boundary conditions

$$\begin{aligned}\lim_{x_1 \uparrow y_1} E(x_1,y_1;x_2,y_2) &= E(x_2,y_2) \\ \lim_{y_1 \uparrow x_2} E(x_1,y_1;x_2,y_2) &= E(x_1,y_2) \\ \lim_{x_2 \uparrow y_2} E(x_1,y_1;x_2,y_2) &= E(x_1,y_1)\end{aligned}$$

can be expressed through the single-interval empty probabilities [35]:

$$\begin{aligned}E(1;2) &= E(x_1,y_1)E(x_2,y_2) - E(x_1,x_2)E(y_1,y_2) \\ &\quad + E(x_1,y_2)E(y_1,x_2) \qquad (50)\end{aligned}$$

For our purposes, it suffices to consider a simple subset of empty interval probabilities, namely those with $y_2 = \infty$. We denote $\mathcal{E}(x,y,z) = E(x,y;z,\infty)$, in analogy with notation $\mathcal{E}(z) = E(z,\infty)$ which we used in Sec. II A. Specifying (50) to this setting we get

$$\mathcal{E}(x,y,z) = E(x,y)\mathcal{E}(z) - E(x,z)\mathcal{E}(y) + \mathcal{E}(x)E(y,z) \qquad (51)$$

Applying $\frac{\partial^2}{\partial x \partial z}$ to Eq. (51) and taking the $z \to y$ limit, we find the probability $R(x,y)$ that the two right-most particles are at x and y:

$$\begin{aligned}R(x,y) &= \frac{\partial E(x,y)}{\partial x}\frac{\partial \mathcal{E}(y)}{\partial y} - \mathcal{E}(y)\frac{\partial^2 E(x,y)}{\partial x \partial y} \\ &\quad - c(y)\frac{\partial \mathcal{E}(x)}{\partial x} \qquad (52)\end{aligned}$$

Further, the probability $P_{\rm c}(1)$ to have exactly one particle in the initially empty half-line can be obtained by

integrating the probability density $R(x, y)$:

$$P_c(1) = \int_0^\infty dy \int_{-\infty}^0 dx\, R(x, y) \qquad (53)$$

Computation of the integrals in Eq. (53), detailed in Appendix B, leads to the the announced expression (8).

As a by-product of these calculations, we can determine the probability density $R(x, y)$ that the first and the second right-most particles are located at x and y. Using (52) we can express $R(x, y)$ in the scaling form

$$R(x, y|t) = \frac{1}{\pi\sqrt{32}}\,(Dt)^{-1}\,\mathcal{R}(X, Y) \qquad (54a)$$

$$\mathcal{R}(X, Y) = e^{-(Y-X)^2/4}\,\mathrm{Erfc}\left(\tfrac{X+Y}{2}\right)\Psi(X, Y)$$
$$- e^{-X^2/2}\,\mathrm{Erfc}(Y) \qquad (54b)$$

where we have used the shorthand notation

$$\Psi(X, Y) = e^{-Y^2/2} + (Y-X)\sqrt{2\pi}\left[1 - \tfrac{1}{2}\mathrm{Erfc}\left(\tfrac{Y}{\sqrt{2}}\right)\right]$$

For the homogeneous coalescence process, the distribution of distance between adjacent particles is easy to determine, see e.g. [12, 13]. For the particles on the edge, however, the computation is involved and the scaled distance distribution (54b) apparently has not been known. For the annihilation process, even in the bulk (equivalently for the homogeneous setting) the distance distribution has not been established despite of the considerable effort [27–29].

B. Simulation Results

We performed numerical simulations to measure various statistical properties including in particular, those of the total number of particle N. In the simulations, we considered the lattice version of the diffusion-controlled coalesce and annihilation processes. Namely, we assumed that particles undergo (continuous time) random walk on the one-dimensional lattice, and instantaneously coalesce (or annihilate) whenever two particles occupy the same site. In the long-time limit, the continuous (with particles undergoing Brownian motion) and the lattice versions lead to the same results.

The initial condition become irrelevant in the long time limit, so we considered the simplest initial condition when half lattice is fully occupied. Thus initially every lattice site in the half-line $x < 0$ is occupied and every lattice site in the half-line $x \geq 0$ is empty.

We measured the stationary distributions $P_a(N)$ and $P_c(N)$ for the number of particles in the initially-empty half space ($x > 0$) in the annihilation and coalescence processes. The results are listed in Table I. The numerical findings are consistent with the sum rule (33), viz. $\sum_{k\geq0} P_a(2k) = \frac{3}{4}$. For the coalescence process, simulation results for $P_c(0)$ and $P_c(1)$ are in excellent agreement with theoretical predictions (46) and (8). The simulation

N	$P_a(N)$	$P_c(N)$
0	0.74	0.50
1	0.25	0.46
2	0.008	0.03
3	$3 \cdot 10^{-5}$	$3 \cdot 10^{-4}$

TABLE I: The probabilities $P_a(N)$ and $P_c(N)$ for $N \leq 3$ as obtained from numerical simulations.
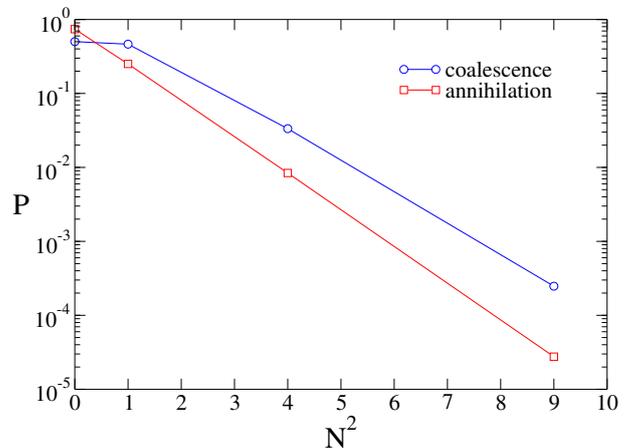

FIG. 4: Semi-logarithmic plots of the distributions $P_a(N)$ and $P_c(N)$ versus N^2.

result for $P_c(2)$ is close to the theoretical upper bound (48) which is natural since $P_c(3)$ is very small according to another theoretical upper bound (49). Both distributions $P_a(N)$ and $P_c(N)$ apparently have Gaussian tails. The numerical evidence (see Fig. 4) looks fairly conclusive, even though the range in N is very small.

C. Characteristics of the leader

Here we outline what we know about the position of the "leader" defined as the right-most particle. Features of interest include its average location $\langle\ell\rangle$, the probability density $\Pi(\ell, t)$ that the leader is at position ℓ at time t, etc. For the coalescence process

$$\langle\ell\rangle_c = 0, \quad \Pi_c(\ell, t) = \frac{1}{\sqrt{4\pi Dt}}\,\exp\left[-\frac{\ell^2}{4Dt}\right] \qquad (55)$$

For the annihilation process, in contrast, $\langle\ell\rangle_a$ and $\Pi_a(\ell, t)$ are not known. Since the initially empty half-line is empty with probability exceeding $\frac{1}{2}$, one anticipates that the average position of the leading particle recedes diffusively into the initially occupied half-line. This was indeed observed in simulations [32] where the probability density $\Pi_a(\ell, t)$ was also measured, and found to be asymmetric and clearly non-Gaussian [32].

We studied numerically the one-dimensional aggregation process (3) with mass-independent diffusion coefficients. We observed that the average mass of the leader

(the right-most aggregate) grows as $\langle m \rangle = B\rho\sqrt{Dt}$ with $B = 1.6 \pm 0.1$. This growth is anticipated, e.g., using (34) one finds that the average total mass in the initially empty half-line grows as $\rho\sqrt{Dt/(4\pi)}$.

The one-dimensional aggregation process generalizes the coalescence process, so it is more tractable than the annihilation process. The properties of the leader might be amenable to exact analysis. We already know the probability density $\Pi_c(\ell, t)$ for its location. It will be interesting to determine the mass distribution $P(m, t)$ and the more detailed joint distribution $\Pi(\ell, m, t)$, i.e., the probability density that the leading particle has mass m and located at ℓ.

IV. DISCUSSION

In summary, we studied three basic one-dimensional diffusion-controlled reaction processes—annihilation, coalescence, and aggregation. In the case of aggregation, we assumed that the diffusion coefficients are mass-independent, so it reduces to the coalescence process if one focuses only on the total cluster distribution. Our theoretical analysis generalizes the empty interval method to inhomogeneous initial conditions.

We examined the evolution starting with the inhomogeneous initial configuration when a half-line is uniformly filled by particles, while the complementary half-line is empty. We computed the average particle density as a function of position. Our main finding is that while the overall density profile is a time-dependent quantity, statistical properties of the total number of particles residing in the initially-empty half-space become independent of time, in the long-time limit. In particular, the total number of particles in the initially empty half-line is finite and governed by a stationary probability distribution. We were able to compute analytically several features of this distribution function, e.g. the average.

There are numerous basic questions about the behavior of one-dimensional diffusion-controlled annihilation, coalescence, and aggregation that remain unanswered. We limited ourselves to equal-time correlation functions. Many of them, e.g. $\langle N(t) \rangle$, become time-independent in the long time limit. Two-time correlation functions, such as $\langle N(t_1)N(t_2) \rangle$, are natural extensions of our study.

Another interesting time-dependent quantities are various first-passage (or persistence) characteristics [40, 41]. For instance, the survival probabilities of the particles in the annihilation process decay algebraically with time; the decay exponent depends only on the parity of the label corresponding to the initial location and these two exponents [32] haven't been determined analytically.

One can also ask about the probability $S(t)$ that not a single particle ever entered the initially empty half-line during the time interval $(0, t)$. For the coalescence process $S_c(t) \sim t^{-1/2}$ since the problem reduces to the survival probability for a Brownian particle in one dimension [40, 41]. For the annihilation process $S_a(t) \sim t^{-3/16}$ as follows from equivalence with a basic persistence problem [42]. The probability of never entering the initially empty half-line is equivalent to the probability that the position of the leader satisfies $\ell(t') < 0$ for all $t' < t$. Since the typical position of the leader scales diffusively, it is natural to ask about the probability that $\ell(t') < A\sqrt{Dt'}$ for all $t' < t$, where A is some fixed constant. This probability decays algebraically, $S(t, A) \sim t^{-\theta(A)}$ as $t \to \infty$. For the coalescence process we have effectively a single particle problem which is solvable and the exponent $\theta_c(A)$ is known [43] for arbitrary A; for the annihilation process, only $\theta_a(0) = \frac{3}{16}$ is known [42]. Another natural generalization involves first-passage properties involving the number of particles residing in the initially-empty half space [44].

In our view, establishing analytical tools for probing the annihilation process represent the most important and most challenging extension of the current work. Some delicate properties of the homogenous annihilation process have been derived analytically [42] using field-theoretical methods; perhaps, the techniques of [42] can be extended to the inhomogeneous setting.

[1] M. V. Smoluchowski, Z. Phys. Chem. **92**, 129 (1917); *ibid* **92**, 155 (1917).
[2] R. Zsigmondy, Z. Phys. Chem. **92**, 600 (1917).
[3] S. Chandrasekhar, Rev. Mod. Phys. **15**, 1 (1943).
[4] R. L. Drake, in: *Topics in Current Aerosol Researches*, eds. G. M. Hidy and J. R. Brock (Pergamon Press, New York, 1972), pp. 201.
[5] S. K. Frielander, *Smoke, Dust and Haze: Fundamentals of Aerosol Behavior* (Wiley, New York, 1977).
[6] M. Bramson and D. Griffeath, Z. Wahrsch. Verw. Geb. **53**, 183 (1980).
[7] R. Arratia, Ann. Probab. **9**, 909 (1981).
[8] A. A. Ovchinnikov, S. F. Timashev, and A. A. Belyi, *Ki-netics of Diffusion Controlled Chemical Processes* (Nova Science Pub. Inc., 1989).
[9] H. Pruppacher and J. Klett, *Microphysics of Clouds and Precipitations* (Kluwer, Dordrecht, 1998).
[10] D. ben-Avraham, M. A. Burschka, and C. R. Doering, J. Stat. Phys. **60**, 695 (1990).
[11] U. C. Tauber, M. Howard, and B. P. Vollmayr-Lee, J. Phys. A **38**, R79 (2005).
[12] D. ben-Avraham and S. Havlin, *Diffusion and Reactions in Fractals and Disordered Systems* (Cambridge University Press, Cambridge, UK, 2000).
[13] P. L. Krapivsky, S. Redner and E. Ben-Naim, *A Kinetic View of Statistical Physics* (Cambridge University Press,

Cambridge, 2010).

[14] E. Brunet and B. Derida, Phys. Rev. E **56**, 2597 (1997).

[15] B. Meerson, A. Vilenkin, P. V. Sasorov, Phys. Rev. E **87**, 012117 (2013).

[16] B. Derrida, J. L. Lebowitz, and E. R. Speer, J. Stat. Phys. **89**, 135 (1997).

[17] U. Schneider, L. Hackermüller, J. P. Ronzheimer, S. Will, S. Braun, T. Best et al., Nature Phys. **8**, 213 (2012).

[18] J. P. Ronzheimer, M. Schreiber, S. Braun, S. S. Hodgman et al., Phys. Rev. Lett. **110**, 205301 (2013).

[19] M. Rigol and A. Muramatsu, Phys. Rev. Lett. **94**, 240403 (2005).

[20] D. M. Gangardt and M. Pustilnik, Phys. Rev. A **77**, 041604 (2008).

[21] A. del Campo, Phys. Rev. A **84**, 031606 (2011).

[22] M. Collura and D. Karevski, Phys. Rev. B **89**, 214308 (2014).

[23] T. Antal, P. L. Krapivsky, and A. Rákos, Phys. Rev. E **78**, 061115 (2008).

[24] V. Eisler and Z. Racz, Phys. Rev. Lett. **110**, 060602 (2013).

[25] T. Sabetta and G. Misguich, Phys. Rev. B **88**, 245114 (2013).

[26] V. Alba and F. Heidrich-Meisner, Phys. Rev. B **90**, 075144 (2014).

[27] P. A. Alemany and D. ben-Avraham, Phys. Lett. A **206**, 18 (1995).

[28] B. Derrida and R. Zeitak, Phys. Rev. E **54**, 2513 (1996).

[29] P. L. Krapivsky and E. Ben-Naim, Phys. Rev. E **56**, 3788 (1997).

[30] P. L. Krapivsky, E. Ben-Naim, and S. Redner, Phys. Rev. E **50**, 2474 (1994).

[31] C. Monthus, Phys. Rev. E **54**, 4844 (1996).

[32] L. Frachebourg, P. L. Krapivsky, and S. Redner, J. Phys. A **31**, 2791 (1998).

[33] B. R. Thomson, J. Phys. A **22**, 879 (1989).

[34] P. L. Krapivsky, Physica A **198**, 150 (1993).

[35] T. O. Masser and D. ben-Avraham, Phys. Rev. E **64**, 062101 (2001).

[36] M. Henkel, E. Orlandini, and G. M. Schütz, J. Phys. A **28**, 6335 (1995).

[37] K. Krebs, M. P. Pfanmüller, B. Wehefritz, and H. Hinrichsen, J. Stat. Phys. **78**, 1429 (1995).

[38] D. Balboni, P.-A. Rey, and M. Droz, Phys. Rev. E **52**, 6220 (1995).

[39] H. Simon, J. Phys. A **28**, 6585 (1995).

[40] S. Redner, *A Guide to First-Passage Processes* (Cambridge University Press, Cambridge, 2001).

[41] A. J. Bray, S. N. Majumdar, and G. Schehr, Adv. Phys. **62**, 225 (2013).

[42] B. Derrida, V. Hakim, and V. Pasquier, Phys. Rev. Lett. **75**, 751 (1995); J. Stat. Phys. **85**, 763 (1996).

[43] P. L. Krapivsky and S. Redner, Am. J. Phys. **64**, 546 (1996).

[44] E. Ben-Naim and P. L. Krapivsky, J. Phys. A **43**, 495007 (2010); J. Phys. A **43**, 495008 (2010).

Appendix A: Scaling Behavior in the One-Dimensional Aggregation Process

One can try to solve (35) using the generating function technique. Here we use another approach relying on the recurrent nature of Eqs. (35). We first show in detail how to find the density of monomers and then generalize. The probability $P_1(x, y; t)$ that the total mass contained in the interval $[x, y]$ is equal to one is clearly the probability that the interval $[x, y]$ contains one monomer. This probability varies according to diffusion equation

$$\frac{\partial}{\partial t} P_1 = D \left(\frac{\partial^2}{\partial x^2} + \frac{\partial^2}{\partial y^2} \right) P_1 \qquad (A1)$$

supplemented by the boundary condition

$$P_1(x, x; t) = 0 \qquad (A2)$$

As earlier, we extend the definition of $P_1(x, y; t)$ from the physically relevant half-plane $x \leq y$ to the entire plane. The initial condition

$$P_1(t=0) = \begin{cases} 0 & x > 0, \ y > 0 \\ (-\rho x)\, e^{\rho x} & x < 0 < y \\ \rho y\, e^{\rho y} & y < 0 < x \\ \rho(y-x)\, e^{\rho(x-y)} & x < y < 0 \\ -\rho(x-y)\, e^{\rho(y-x)} & y < x < 0 \end{cases} \qquad (A3)$$

agrees with (38) when $x \leq y$, while in the supplementary half-plane $x \geq y$ the choice made in Eq. (A3) assures that the boundary condition (A2) is manifestly obeyed.

Solving the diffusion equation (A1) subject to the initial condition (A3) yields

$$\begin{aligned} \frac{4\pi Dt}{\rho} P_1 &= \int_{-\infty}^{0} dx_0 \int_{0}^{\infty} dy_0 \, (-x_0)\, e^{\rho x_0} G \\ &+ \int_{0}^{\infty} dx_0 \int_{-\infty}^{0} dy_0 \, y_0 \, e^{\rho y_0} G \\ &+ \int_{-\infty}^{0} dy_0 \int_{-\infty}^{y_0} dx_0 \, (y_0 - x_0)\, e^{\rho(x_0 - y_0)} G \\ &+ \int_{-\infty}^{0} dx_0 \int_{-\infty}^{x_0} dy_0 \, (y_0 - x_0)\, e^{-\rho(x_0 - y_0)} G \end{aligned}$$

Here $G = G(x, y, t | x_0, y_0)$ is the diffusion propagator:

$$G(x, y, t | x_0, y_0) = \exp\left\{ -\frac{(x - x_0)^2 + (y - y_0)^2}{4Dt} \right\}$$

Recalling (37) and performing straightforward calculations one finds the monomer density $c_1(x, t)$

$$\begin{aligned} \frac{8\pi (Dt)^2}{\rho} c_1 &= \int_{0}^{\infty} dy_0 \int_{0}^{\infty} dw \, w^2 e^{-\rho w} H_1 \qquad (A4) \\ &+ \int_{0}^{\infty} dy_0 \int_{0}^{\infty} dx_0 \, x_0 e^{-\rho x_0} (y_0 - x_0) H_2 \end{aligned}$$

where we have used shorthand notation:

$$\begin{aligned} H_1 &= H(x|-y_0, -y_0 - w) \\ H_2 &= H(x|-x_0, y_0) \\ H(x|x_0, y_0) &= \exp\left\{ -\frac{(x - x_0)^2 + (x - y_0)^2}{4Dt} \right\} \end{aligned}$$

The integral representation (A4) is exact, that is, valid at all $t > 0$. In the long-time limit, the monomer density simplifies. Let us first compute $c_1(0,t)$, the monomer density exactly on the interface. When $x = 0$, the right-hand side of (A4) becomes

$$\int_0^\infty dy_0 \int_0^\infty dw\, w^2 e^{-\rho w} \exp\left\{-\frac{y_0^2 + (y_0 + w)^2}{4Dt}\right\}$$
$$+ \int_0^\infty dy_0 \int_0^\infty dx_0\, x_0 e^{-\rho x_0}(y_0 - x_0)\exp\left\{-\frac{x_0^2 + y_0^2}{4Dt}\right\}$$

In the long-time limit, more precisely when $\rho^2 Dt \gg 1$, the integral in the second line dominates and asymptotically it grows as $2Dt/\rho^2$. Therefore

$$c_1(0,t) = \frac{1}{4\pi\rho Dt} \tag{A5}$$

More generally, $c_1(x,t) = (4\pi\rho Dt)^{-1/2}$ for $x \sim \rho^{-1}$.

In the scaling limit (5) with X being fixed, the integral in the first line on the right-hand side of (A4) approaches to $\rho^{-3}(2\pi Dt)^{1/2}\,\mathrm{Erfc}(X)$, while the integral in the second line of (A4) tends to

$$\frac{2Dt}{\rho^2}\left[\sqrt{\frac{\pi}{2}}\,Xe^{-X^2/2}\,\mathrm{Erfc}\left(-\frac{X}{\sqrt{2}}\right) + e^{-X^2}\right]$$

Thus

$$c_1(X,t) = \frac{1}{4\pi\rho Dt}\left[\sqrt{\frac{\pi}{2}}\,Xe^{-X^2/2}\,\mathrm{Erfc}\left(-\frac{X}{\sqrt{2}}\right) + e^{-X^2}\right]$$
$$+ \frac{1}{2\rho^2}\frac{1}{\sqrt{8\pi(Dt)^3}}\,\mathrm{Erfc}(X) \tag{A6}$$

The term in the second line is negligible for finite X, both positive and negative, but we kept this term as it prevails when $X \ll -\sqrt{\ln(\rho^2 Dt)}$. This term determines the asymptotic monomer density far away from the interface (equivalently, for the uniform initial distribution):

$$c_1(-\infty,t) = (8\pi)^{-1/2}\,\rho^{-2}\,(Dt)^{-3/2} \tag{A7}$$

A similar treatment other clusters leads to

$$\frac{8\pi(Dt)^2}{\rho^m}c_m = \int_0^\infty dy_0 \int_0^\infty dw\,\frac{w^{m+1}}{m!}\,e^{-\rho w}H_1$$
$$+ \int_0^\infty dx_0 \int_0^\infty dy_0\,\frac{x_0^m}{m!}\,e^{-\rho x_0}(y_0 - x_0)H_2$$

For clusters of finite mass, $m = O(1)$, one gets

$$c_m(X,t) = \frac{1}{4\pi\rho Dt}\left[\sqrt{\frac{\pi}{2}}\,Xe^{-X^2/2}\,\mathrm{Erfc}\left(-\frac{X}{\sqrt{2}}\right) + e^{-X^2}\right]$$
$$+ \frac{m+1}{4\rho^2}\frac{1}{\sqrt{8\pi(Dt)^3}}\,\mathrm{Erfc}(X) \tag{A8}$$

The term in the first line dominates for finite X, and it does *not* depend on the mass in the leading order.

Appendix B: Computation of the integrals in (53)

Plugging (52) into (53) and performing the integration over x we get

$$P_{\mathrm{c}}(1) = \int_0^\infty dy\,\frac{\partial\mathcal{E}(y)}{\partial y}\,[E(0,y) - E(-\infty,y)]$$
$$- \int_0^\infty dy\,\mathcal{E}(y)\,\frac{\partial}{\partial y}\,[E(0,y) - E(-\infty,y)]$$
$$- \int_0^\infty dy\,c(y)[\mathcal{E}(0) - \mathcal{E}(-\infty)] \tag{B1}$$

Since $E(-\infty,y) = \mathcal{E}(-\infty) = 0$ and $\mathcal{E}(0) = \frac{1}{2}$ we have

$$P_{\mathrm{c}}(1) = \int_0^\infty dy\left[\frac{\partial\mathcal{E}(y)}{\partial y}\,E(0,y) - \mathcal{E}(y)\,\frac{\partial E(0,y)}{\partial y}\right]$$
$$- \frac{1}{2}\int_0^\infty dy\,c(y) \tag{B2}$$

Integrating by parts, we simplify (B2) to

$$P_{\mathrm{c}}(1) = 2\int_0^\infty dy\,\frac{\partial\mathcal{E}(y)}{\partial y}\,E(0,y) - \frac{1}{2}\int_0^\infty dy\,c(y) \tag{B3}$$

Specifying (25) to $x = 0$, we get

$$E(0,y) = 1 - \tfrac{1}{2}\mathrm{Erfc}\left(\tfrac{Y}{2}\right)\mathrm{Erf}\left(\tfrac{Y}{2}\right)$$
$$- \frac{1}{\pi}\int_{-\frac{Y}{2}}^\infty du\,e^{-u^2}\int_u^{u+Y} dv\,e^{-v^2}$$

Expressing the integral through error functions yields

$$E(0,y) = 1 - \tfrac{1}{2}\mathrm{Erf}\left(\tfrac{Y}{2}\right) + \tfrac{1}{4}\left[\mathrm{Erf}\left(\tfrac{Y}{2}\right)\right]^2 - \tfrac{1}{4}\mathrm{Erf}\left(\tfrac{Y}{\sqrt{2}}\right)$$

It is convenient to transform y to Y in the first integral in (B3). Equation (27) gives $dy\,\frac{\partial\mathcal{E}(y)}{\partial y} = dY\,\frac{1}{\sqrt{2\pi}}\,e^{-Y^2/2}$. The above results together with $\int_0^\infty dy\,c(y) = \langle N\rangle_{\mathrm{c}}$, see (44), allow us to re-write (B3) as

$$P_{\mathrm{c}}(1) = \sqrt{\frac{8}{\pi}}\int_0^\infty dz\,e^{-2z^2}\,\Pi(z) - \frac{1}{2}\langle N\rangle_{\mathrm{c}} \tag{B4}$$

with

$$\Pi(z) = 1 - \tfrac{1}{2}\mathrm{Erf}(z) + \tfrac{1}{4}[\mathrm{Erf}(z)]^2 - \tfrac{1}{4}\mathrm{Erf}(\sqrt{2}\,z)$$

Computing the integrals in (B4) one gets

$$\sqrt{\frac{8}{\pi}}\int_0^\infty dz\,e^{-2z^2} = 1$$
$$\sqrt{\frac{8}{\pi}}\int_0^\infty dz\,e^{-2z^2}\,\mathrm{Erf}(z) = \frac{2}{\pi}\arctan\left(\frac{1}{\sqrt{2}}\right)$$
$$\sqrt{\frac{8}{\pi}}\int_0^\infty dz\,e^{-2z^2}\,\mathrm{Erf}(\sqrt{2}\,z) = \frac{1}{2}$$
$$\sqrt{\frac{8}{\pi}}\int_0^\infty dz\,e^{-2z^2}\,[\mathrm{Erf}(z)]^2 = \frac{2}{\pi}\arctan\left(\frac{1}{\sqrt{8}}\right)$$

Using these expressions and recalling (7) we reduce (B4) to the announced result (8).